20

Development of Test-Bed AUV 'ISiMI' and Underwater Experiments on Free Running and Vision Guided Docking

Jin-Yeong Park[1], Bong-huan Jun[2], Pan-mook Lee[2] and Junho Oh[1]
[1]*Humanoid Robot Research Center, KAIST*
[2]*Ocean Engineering Research Department, MOERI, KORDI*
Republic of Korea

1. Introduction

In this chapter, development of a test-bed AUV is described. Free running test and vision guided docking are also presented.

Autonomous underwater vehicles (AUVs) have become a main tool for surveying below the sea in scientific, military, and commercial applications because of the significant improvement in their performance. Despite the considerable improvement in AUV performance, however, AUV technologies are still attractive to scientists and engineers as a challenging field. For example, multiple AUVs and underwater docking are recent challenging issues in the field of AUV technologies (Edwards et al., 2004; Fiorelli et al., 2004; Stokey et al., 2001; Singh et al., 2001). To successfully implement these new technologies in the field, a number of sub-functions have to be tested and verified in advance. They could be control, navigation and communication functions as well as basic functions for AUVs, including an emergency architecture for survival. Since it would be very expensive and time consuming to conduct all these tests at sea, researchers and engineers engaged in the operation and development of underwater vehicles need easier test schemes and faster feedback of results in an environment similar to that of the sea.

Underwater docking of an AUV to a launcher without surfacing allows the AUV have longer and more frequent investigations. Data uploading, mission downloading and recharge of batteries are essential duties of docking systems. Many research institutes have developed docking systems for AUVs. An ElectroMagnetic homing (EM) system was proposed as one of them (Feezor et al., 1997). A magnetic field generated by coils on the dock was used in that system. An AUV sensed this magnetic field and was guided to the dock. The range of the EM system was limited to 25-30m. An optical terminal guidance system was also introduced (Cowen et al., 1997). That system was simple but highly effective. The optical docking system provided targeting accuracy on the order of 1 cm under real-world conditions, even in turbid bay water. Autonomous docking demonstrations using an ultra-short baseline (USBL) acoustic homing array were shown in (Allen et al., 2006). The acoustic system was capable of acquiring a dock-mounted transponder at ranges of 3,000m or more.

Source: Underwater Vehicles, Book edited by: Alexander V. Inzartsev,
ISBN 978-953-7619-49-7, pp. 582, December 2008, I-Tech, Vienna, Austria

The superiority of the vision system was described in Deltheil et al. (2000). Deltheil et al. (2000) introduced simulations of an optical guidance system for recovery of an unmanned underwater vehicle (UUV). Acoustic, magnetic and optical sensing methods were compared. It was shown that the optical method is superior and the best choice for the UUV recovery guidance system. Vision systems can be easy to operate, robust and fast analyzing (Deltheil et al., 2000). Lee et al. (2002) suggested a visual servo control algorithm using one camera and an optical flow equation. The optical flow equation was combined with the linearized equations of motion of an AUV. They derived a state equation for the visual servoing AUV. They supposed that a charge-coupled device (CCD) camera was installed at the nose of an AUV. Hong et al. (2003) introduced an algorithm for how to estimate relative pose and relative position between an AUV and an underwater dock. They supposed that lights were arranged on the circular rim of the entrance to the dock. Then, the lights were projected as an ellipse on the camera image plane. The geometric and perspective relationship of the circle in 3-dimension space and the ellipse in a projected 2-dimension plane were used in that scheme. From the geometric shape of the ellipse, relative distance and relative pose were estimated. One shortcoming of the above research is that, there were no underwater experiments to verify the algorithms in Deltheil et al., (2000) or Hong et al., (2003).

The Maritime and Ocean Engineering Research Institute (MOERI), a branch of the Korea Ocean Research and Development Institute (KORDI), has developed a model for an AUV named ISiMI. ISiMI comes from the name of a small but strong fish from an old traditional story in Korea. In English, ISiMI is the acronym for Integrated Submergible for Intelligent Mission Implementation. ISiMI is an AUV platform that satisfies the various needs of the experimental tests required for the development of control and navigational architectures or software algorithms for underwater flying vehicles. To carry out a number of tests while avoiding many difficulties in field trials, the first version of ISiMI was designed to cruise in the Ocean Engineering Basin (OEB), a facility in KORDI that simulates the ocean's environment.

A series of free running tests was conducted to investigate the dynamic characteristics of ISiMI and to validate its various functions as a test-bed AUV. These tests included a turning test, a zigzag test, an automatic heading test, a depth control test and a guidance control test. The experimental responses were analyzed and compared with the simulation responses to verify the discrepancies between the two sets of results.

This chapter presents a review of our research work on the development of the AUV ISiMI and its performance evaluation, by simulations and experimental tests. First, the design and implementation of ISiMI, including its positioning system in the OEB, will be presented. Second, a series of test results in the basin and a discussion of the results will be presented, with comparisons of the simulated and experimental outputs. Finally, the second generation ISiMI, ISiMI100, a sea-trial version of ISiMI, will be introduced.

This chapter also presents a final approach algorithm for underwater docking based on vision-guidance, as well as its experimental realization. Configuration of the vision-guidance system for ISiMI will be described. Next, the image processing method used to discriminate an underwater dock is explained. The arrangement of the lights on the dock and how to estimate the center of the dock from the position of the lights is described. The final approach algorithm guides the AUV from when it reaches a distance of 10-15m away of the dock until it reaches the dock. It generates reference yaw and reference pitch from the

estimated center and allows the AUV to track them. Underwater docking experiments are also introduced. The overall system validity was investigated and the final approach algorithm was verified. There was a position where the lights on the dock were outside of the camera viewing range when the AUV was close to the dock. It was expected that the vision-guidance would be invalid in this area. It was also expected that an algorithm based only on vision-guidance would be insufficient in the underwater experiments. Hence, an auxiliary method for precisely guiding the AUV in the area close to the dock is also suggested.

2. System design of the ISiMI AUV

2.1 Basic design concept

The basic design concept of the AUV ISiMI is hinged on the implementation of a small vehicle that can be easily launched, recovered and operated without special handling equipment. This concept of a small AUV is intended to provide researchers with fast experimental feedback on new algorithms and instruments necessary to develop AUV technologies. Several AUVs were reviewed to lead the concept of ISiMI. Sea Squirt AUV, which is 1m long and weighs 35 kg, was built in 1988 under the MIT Sea Grant to gather oceanographic data from the Charles River and serve as a test-bed for software and instrumentation, with component costs of $40,000. Then the MIT Sea Grant built Odyssey I and II for oceanographic research, with component costs of $50,000 and $75,000, respectively (Bellingham et al., 1993). Hydroid's REMUS (Allen et al., 1997; Stokey et al., 2001) and GAVIA AUV, developed by WHOI and Hafmynd, respectively, are small commercially available AUVs with diameters less than 25 cm.

MOERI-KORDI has a big square basin, OEB, for simulation of real sea conditions. OEB is 68.8m long, 37.2m wide and 4.5m deep. Wave, current and wind generators are installed in the basin. The purpose of ISiMI is to serve as a test-bed AUV for the development of AUV technologies with fast experimental feedback in an OEB environment. The size of ISiMI is constrained by the OEB environment, so ISiMI is able to run free in OEB. Its downsizing is at the highest level of the design process. Because the dimensions of the AUV conflict with the space and payload for instruments, however, the hull size and weight of ISiMI were determined in the spiral design process, which is a feedback design from the basic design to the detailed design.

In general, the hull shape of AUVs has mainly two types. The first is the cruising type, which looks like a torpedo, and which surveys from hundreds of meters to hundreds of kilometers. Its streamlined shape is adopted for AUVs to minimize the drag forces acting on the hull while the AUV is cruising. They use axial thrusters and control planes to control their motion. The other type of hull shape is the hovering type, which inspects a specific area from several meters to hundreds of meters. Several thrusters are installed to keep their precise positions and attitudes in hovering motion. Since ISiMI is a test-bed for underwater survey and docking technologies, the torpedo-type hull shape was adopted. Moreover, a pressure hull structure was chosen rather than an open frame structure for spatial efficiency.

2.2 Design goal

Considering ISiMI's basic design concept, we formulated its design goals as follows:

1. *Downsizing:* Its weight had to be 20–30 kg, including payloads for additional sensors or instruments. This scale can be handled by one or two people.

2. *Operating speed and duration:* The vehicle must have been able to operate for more than 3 h at a speed greater than two knots.
3. *Hull shape:* The hull had to have an experimentally known shape that would make it convenient to estimate the hydrodynamic coefficients of a mathematical model and that would minimize the drag force to increase the efficiency of the AUV's thrust. It also had to have space for additional instruments and to endure a depth rating of more than 20m.
4. *Computing and processing power:* The AUV's embedded computer system had to have enough computing power to process navigational and control algorithms and to gather data.
5. *Reliability and compatibility:* The system had to employ proven equipment to minimize the faults of subsystems and to increase the reliability of the entire system. The equipment had to be chosen from among the vendor-supplied instruments continuously and stably.
6. *Extendability*: The AUV had to have the capacity to have additional functions with minimal changes in the basic design of its mechanical and electrical systems.

3. System implementation of ISiMI AUV

3.1 Overview of ISiMI

In the consideration of the design concept, a first version of ISiMI was manufactured with fundamental sensors that were required to enable it to cruise in the OEB. The appearance of ISiMI is shown in Fig. 1. Adopting the modular design concept, we can insert additional mission sensors by extending the length of the AUV's mid-section hull. Fig. 2 shows the ISiMI hull that was extended by inserting an acoustic telemetry module, and Table 1 shows a comparison of the principal dimensions of ISiMI and the extended ISiMI. This chapter

Fig. 1. Appearance of ISiMI AUV

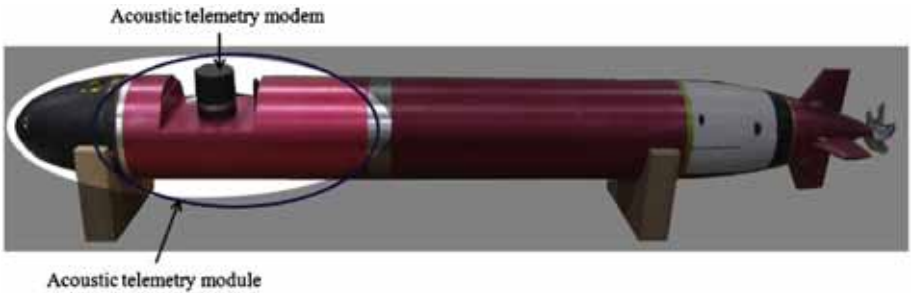

Fig. 2. Acoustic telemetry module

focuses on the first version of ISiMI AUV to cruise in the OEB. The ISiMI system is divided into a mechanical system, a control system and a communication system. Its mechanical

system includes its hull structure, its thruster and its control fins. Its control system includes a computer, electrical interface boards, sensors and software. Its communication system, which enables it to communicate with surface or other vehicles, includes wired and wireless LAN and a R/F modem. The extended ISiMI has an acoustic modem for underwater wireless communication. A new generation ISiMI100 will be equipped with a hybrid navigation system composed of an inertial measurement unit, a Doppler velocity log and range information (Lee et al., 2007; Lee and Jun, 2007).

Symbol	ISiMI	ISiMI100	Unit	Description
L	1196	1582	mm	Overall length
D	170	200	mm	Diameter
W	15	38	kg	Weight
U	1.0	1.5	m/s	Design velocity
u_{max}	2.0	2.0	m/s	Max velocity

Table 1. Dimensions of ISiMI

3.2 Mechanical system

The hull size of the ISiMI AUV is constrained by the space for the onboard instruments, and the hull shape is constrained by the AUV's hydrodynamic characteristics. The standard hull length and diameter are 1.2 and 0.17 m, respectively, considering the installation of the onboard equipment, which will be described in the following sections. The hull shape of the ISiMI AUV was designed based on the Myring hull profile equations (Myring, 1976), which are known as the best contours for minimizing the drag coefficient for a given ratio of body length and diameter. The dimensions of the ISiMI AUV are shown in Table 2. Its hull contour is shown in Figs. 3. Its mid-section is a pressure housing made of aluminum, and its nose section is a flooding hull made of polyurethane. Its tail-section tube, which includes a mounting jig for a BLDC motor and three linear actuators, is covered by a buoyant material. The NACA 0012 cross-section was adopted for the control plane. The design parameters are listed in Table 3. Linear stepper motors were chosen for the fin actuators. The pair of rudders is controlled by a linear stepper motor, and the two stern elevators are independently driven by two linear stepper motors. Assuming the maximum torque required by the control fin is 10 kg cm, including the torque margin for mechanical loss, and assuming that the distance between the fin shaft and the driving axis is 5 cm, we chose a 25N stepper motor for each elevator and a 50N motor for the rudders. The capacity of the thruster motor was estimated based on the drag equation, described as

$$F_d = -\frac{1}{2} C_d \rho A_f u|u| \tag{1}$$

wherein F_d is the form drag acting on the hull, C_d is the drag coefficient, A_f is the maximum cross-sectional area of the hull, u is the advanced speed, and ρ is the water density. The required power capacity was obtained using:

$$P_M = -\frac{1}{2} C_d \rho A_f u|u| \cdot \eta \cdot u \tag{1}$$

wherein P_M is the estimated power capacity of the thrust motor, and η is the total efficiency, including the motor efficiency, the mechanical efficiency (including the friction loss), and the propeller efficiency. The calculation results are shown in Table 4 when the total efficiency was reduced to 0.4. To achieve more than the maximum design speed, an 80-watt BLDC motor with a reduction gear with a 5.8:1 gear ratio (made by Maxon Motors) was selected as the thruster motor. The selected propeller for the thrust system was KP452 S175, from the KORDI propeller series.

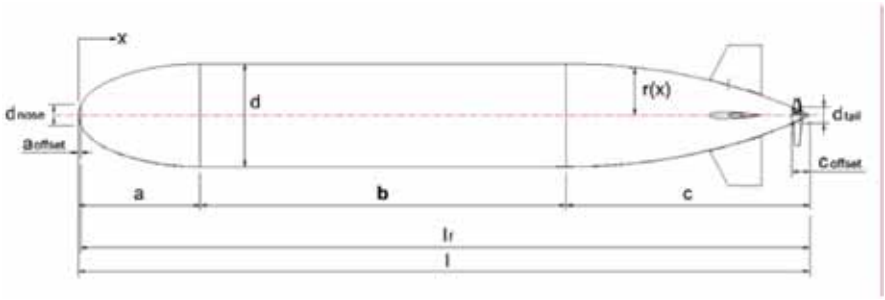

Fig. 3. Hull contour of ISiMI AUV.

Parameters	Value	Unit	Description	Remark
a	200	mm	Nose section	
b	600	mm	Mid-section	
c	400	mm	Tail section	
D	170	mm	Diameter	
a_{offset}	4	mm	Nose offset	
b_{offset}	30	mm	Tail offset	
l_f	1196	mm	Forward length	
l	1200	mm	Total length	

Table 2. Hull parameters of IsiMI

Parameters	Value	Unit	Description	Remark
S_{fin}	4819.5	mm^2	Planform area	
$X_{finpost}$	550	mm	Moment art wrt CB	
δ_{max}	20	degress	Maximum fin angle	

Table 3. Fin parameter of ISiMI

Speed	1m/s	1.5m/s	2m/s	2.5m/s
F_d(N)	2.2698	5.1071	9.0792	14.1867
P_d(W)	2.2698	7.6608	18.1584	35.4656
P_M(W)	5.6745	19.1514	45.3960	88.6641

Table 4. Drag force and required capacity of thrust motor for ISiMI AUV at Re = 1.6E+6, d = 0.17mm, C_d = 0.2, σ = 1.00E+03

3.3 Control System

The standard sensors of ISiMI include an AHRS (attitude heading reference system), a pressure sensor, a CCD camera, and a voltage sensor to check the battery voltage. The AHRS supplies information on the 3-axis angular velocities, 3-axis accelerations, 2-axis inclinations, and heading to the control system. The depth information is gathered from the pressure sensor. A CCD camera mounted on the nose is used to detect the underwater dock at the final stage of the underwater docking for the terminal guidance.

The general arrangement of the parts of ISiMI is shown in Fig. 6. The core of ISiMI's control system is a single-board computer interfaced with a frame grabber, a serial extension board, and a controller area network (CAN) module via a PC104 bus. Figure 4 shows a block diagram of ISiMI's control system. The operating system of the main computer is Windows XP, with real-time extension (RTX). The application software for the graphic user interface and the dynamic control of ISiMI is implemented with Visual C++. To interface sensors and actuators with the main controller, a sub-controller using a Micro Controller Unit (MCU) was developed. The sub-controller communicated with the main controller via a CAN. It controlled the linear actuators and digital and analog I/O intraface. A block diagram of the sub-controller is shown in Fig. 5. The operating duration of ISiMI was estimated at four hours with lithium-polymer batteries of a 207Wh capacity, as shown in Table 4. The total weight of ISiMI in air is 20 kg, including an additional payload of 5 kg. The CCD camera and the frame grabber constitued a vision-guidance system. Fig. 7 is a block diagram of the vision-guidance system. The CCD camera transmitted the Consultative Committee on International Radio (CCIR) signal to the frame grabber. The frame grabber was a PC/104+ type and grabbed image frames at 10-15 Hz. Specifications for each are shown in Table 5 and Table 6, respectively. The image frames were processed on a Windows timer which was not deterministic. Because the image processing could take a lot of time, it was not possible to do it using a deterministic timer. Results of the image processing were stored in the shared memory. The real-time controller extracted and used the results from the shared memory.

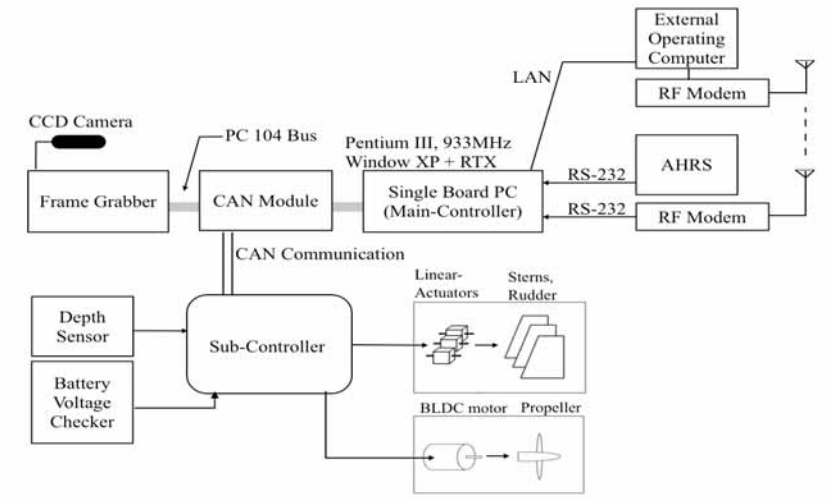

Fig. 4. Control system diagram of ISiMI.

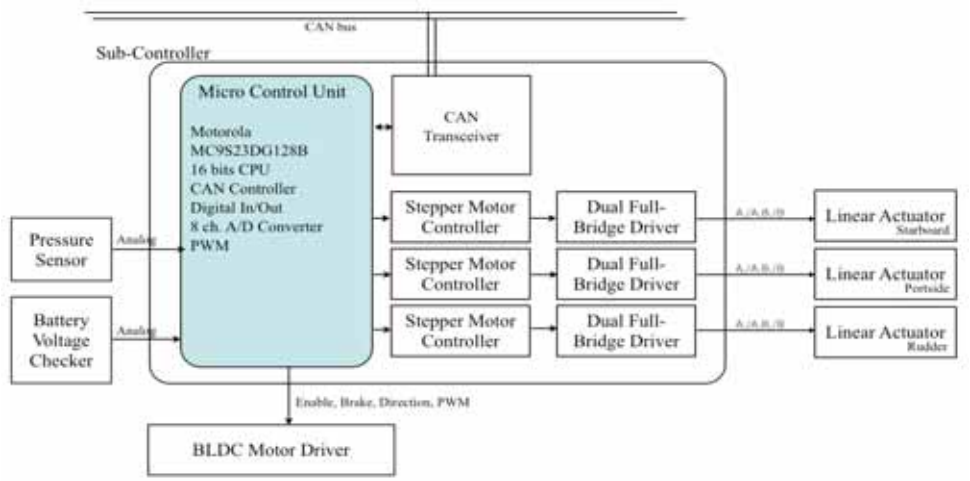

Fig. 5. Sub-controller.

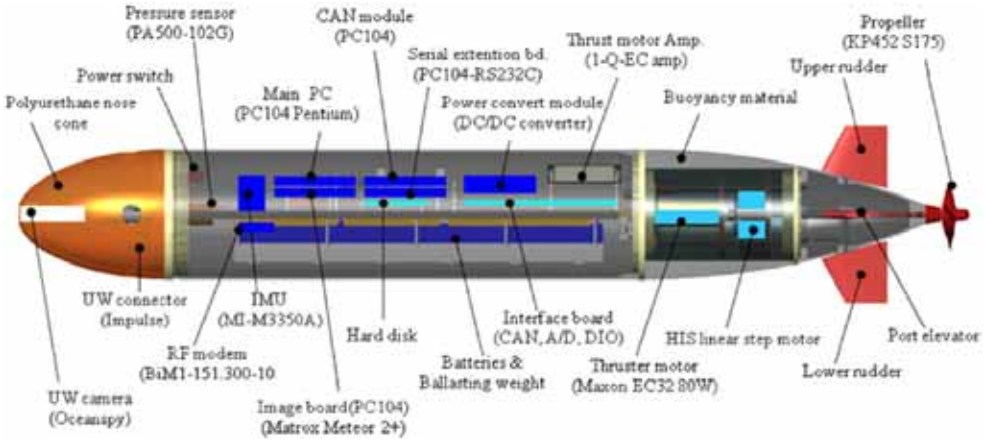

Fig. 6. General arrangement of the AUV ISiMI system.

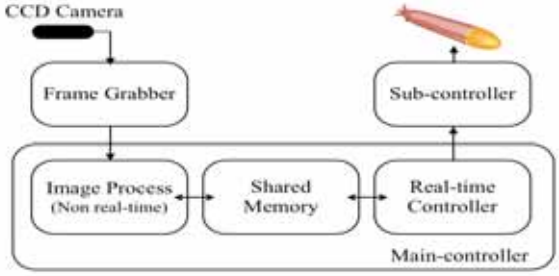

Fig. 7. Block diagram of the vision-guidance system.

Model	OceanSpy
Manufacturer	Tritech
Scanning	2:1 Interlace
Lens	3.6mm F2
Angular view in air	51^o vertical 40^o horizontal
Iris	Auto iris
Operating depth	6,000m water depth
Power	12-30V, 120mA
Dimension	10cm length, 3.4cm diameter

Table 5. Specifications of the CCD camera

Model	Matrox Meteor II+
Manufacturer	Matrox Imaging
Interface	PC/104+
Video source	NTSC, PAL, RS-170, CCIR
Channel	Up to 12 video inputs
Pixel format	RGB 8:8:8 or YU 4:2:2
Dimension	11.56cm length, 9.6cm width

Table 6. Specifications of the frame grabber

3.4 Communication system

A wireless local area network (LAN) was adopted as the communication system between ISiMI and a surface computer, which is used for offline communication for the mission allocation and data downloading. A wired LAN is additionally used as backup. A radio frequency (R/F) modem is installed for online communication between ISiMI and the surface computer for real-time data exchange. Generally, radio frequency cannot be used underwater because of the severe attenuation. We experimentally confirmed, however, that it is practical to transmit packets bi-directionally up to 3.5 meters deep in the OEB with an R/F modem with a bandwidth of 151.3 MHz and an output of 10 mW. With the R/F link, the user's commands and ISiMI's position are transmitted from the surface PC to ISiMI, and acknowledgments of reception are returned to the surface PC.

3.5 Localization in the OEB

The localization problem is a major challenge in underwater robotics. In the OEB environment, there is a severe constraint to using an acoustic positioning system due to the multi-path of the acoustic signal reflected from the wall and bottom of the OEB and from the free surface. Therefore, the image tracking system on the CPMC in the OEB is used for the non-contract position tracking of ISiMI. The CPMC has a three-degrees-of-freedom moving mechanism that enables ISiMI to follow the x-y position and heading of an object located

under the CCD camera. The position and heading of the object with respect to the CCD coordinates are transformed to the reference coordinates (the basin coordinates) using the position and heading of the camera with respect to the reference coordinates, which are calculated from the encoders of the CPMC actuators. The tracked position of ISiMI is transmitted to the ISiMI with a 2Hz bandwidth via a wireless R/F link between the surface computer and ISiMI in real time. The image tracking system installed under CPMC is shown in Fig. 8.

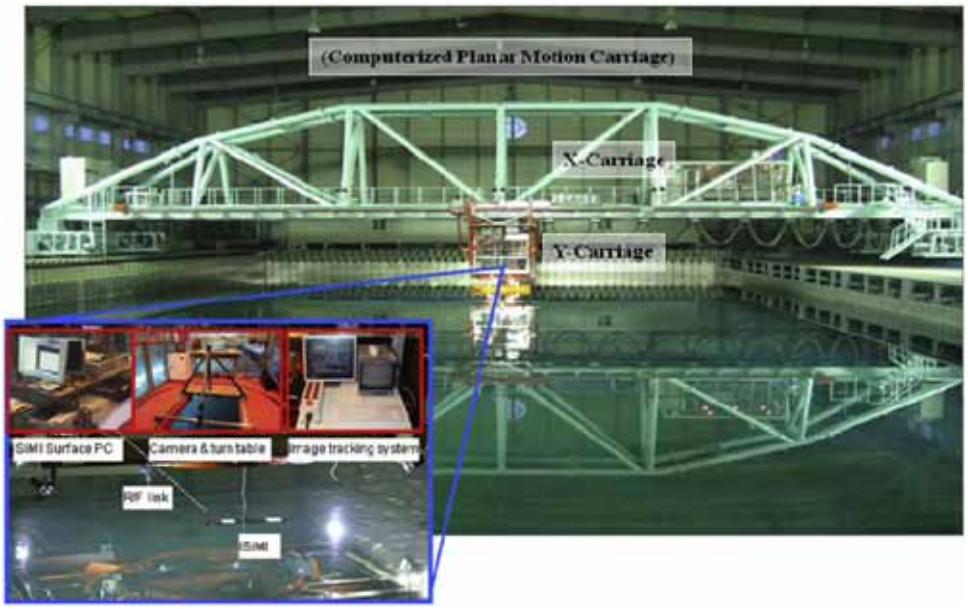

Fig. 8. CPMC and image tracking system of the OEB.

4. Numerical model and controller design

4.1 Numerical model

The three-dimensional non-linear dynamic equation of submersible motion has been described by Gertler and Hagen (1967), Feldman (1979) and Fossen (1994). Ignoring the effect of current, we can describe the dynamic equation of ISiMI as the form in the study of Feldman (1979) or Gertler and Hagen (1967). Considering the body coordinate system in Fig. 9 and classifying the terms in the dynamic equation, we get the following equation for ISiMI:

$$\mathbf{M}\dot{\mathbf{v}} = \mathbf{F}_{CC} + \mathbf{F}_{vh} + \mathbf{F}_{rest} + \mathbf{F}_{thrust} + \mathbf{F}_{fin} \tag{3}$$

wherein $\dot{\mathbf{v}} = \{u, v, w, p, q, r\}^{\mathrm{T}}$ is the linear and angular velocity vector with respect to the body coordinate frame, $\mathbf{M}$ is the inertial term including the added mass, $\mathbf{F}_{CC}$ is the coriolis and centrifugal force term for a rigid body, $\mathbf{F}_{vh}$ is the velocity-dependent hydrodynamic force acting on the body, $\mathbf{F}_{rest}$ is the restoring force, $\mathbf{F}_{thrust}$ is the thrust force, and $\mathbf{F}_{fin}$ is the lift and drag force on the fins. Each element term in (3) is listed in (Jun et al., 2008). The

hydrodynamic coefficients in the model were estimated using the Nernstein and Smith method and the Prestero method. The developed coefficients were non-dimensionalized with the length of the vehicle and are listed in (Jun et al., 2008). The roll damping coefficient was analogized from that of similar vehicles.

$$\dot{\boldsymbol{\eta}}_1 = \mathbf{J}_1(\boldsymbol{\eta}_2)\mathbf{v}_1 \;\Leftrightarrow\; \mathbf{v}_1 = \mathbf{J}_1{}^{-1}(\boldsymbol{\eta}_2)\dot{\boldsymbol{\eta}}_1 \tag{4}$$

$$\dot{\boldsymbol{\eta}}_1 = \mathbf{J}_1(\boldsymbol{\eta}_2)\mathbf{v}_1 \;\Leftrightarrow\; \mathbf{v}_1 = \mathbf{J}_1{}^{-1}(\boldsymbol{\eta}_2)\dot{\boldsymbol{\eta}}_1 \tag{5}$$

The velocity $\mathbf{v}$ in (3) can be written with respect to the earth-fixed coordinate frame with the transformation matrices $\mathbf{J}$ s as follows:

wherein $\mathbf{v}_1 = \{u, v, w\}^{\mathrm{T}}$ and $\mathbf{v}_2 = \{p, q, r\}^{\mathrm{T}}$ are the linear and angular velocities with respect to the body coordinate frame, respectively; $\boldsymbol{\eta}_1 = \{X, Y, Z\}^{\mathrm{T}}$ and $\boldsymbol{\eta}_2 = \{\phi, \theta, \psi\}^{\mathrm{T}}$ are the position and attitude vectors with respect to the earth-fixed frame, respectively; and $\mathbf{J}_1, \mathbf{J}_2$ are the linear and angular velocity transformation matrices referred to in (Jun et al., 2008). Based on the non-linear dynamics of ISiMI, we developed a simulation environment for it using MatLab and Simulink. All the simulation results presented in this chapter were derived from the simulation environment.

4.2 Controller design for free running tests

The sliding mode controller has been successfully applied to the control of underwater vehicles (Healey & Lienard, 1990; Utkin, 1997; and Lee, 1999). The sliding mode controller was used as the motion controller of ISiMI. The simplified equations for the steering and diving motions were derived by ignoring the cross-flow terms and higher-order terms. (Jun et al., 2008) The linearized steering system dynamics are given by:

$$\dot{\mathbf{x}}_h(\mathrm{t}) = \mathbf{A}_h\mathbf{x}_h(\mathrm{t}) + \mathbf{b}_h\delta_R(\mathrm{t}) \tag{6}$$

$$\mathbf{A}_h = \begin{bmatrix} I_z - \frac{\rho}{2}l^5 N_{\dot{r}} & 0 \\ 0 & 1 \end{bmatrix}^{-1} \begin{bmatrix} \frac{\rho}{2}l^4 N_r & 0 \\ 1 & 0 \end{bmatrix}$$

$$\mathbf{b}_h = \begin{bmatrix} I_z - \frac{\rho}{2}l^5 N_{\dot{r}} & 0 \\ 0 & 1 \end{bmatrix}^{-1} \begin{bmatrix} \frac{\rho}{2}l^3 U^2 N_{\delta_R} \\ 0 \end{bmatrix}$$

$$\mathbf{x}_h = \begin{bmatrix} r & \psi \end{bmatrix}^{\mathrm{T}}$$

The sliding poles of the steering system arbitrarily at [0 - 2], we got the steering control law as:

$$\delta_R = -0.0281r + 2.58\eta\tanh\left(r + 2(\psi - \psi_{com})/1\right) \tag{7}$$

The linearized diving system dynamics are given by the third-order system:

$$\dot{\mathbf{x}}_v(\mathrm{t}) = \mathbf{A}_v \mathbf{x}_v(\mathrm{t}) + \mathbf{b}_v \delta_S(\mathrm{t}) \tag{8}$$

$$\mathbf{A}_v = \begin{bmatrix} I_y - \frac{\rho}{2} l^5 M_{\dot{q}} & 0 & 0 \\ 0 & 1 & 0 \\ 0 & 0 & 1 \end{bmatrix}^{-1} \begin{bmatrix} \frac{\rho}{2} l^4 M_q & -z_G W & 0 \\ 1 & 0 & 0 \\ 0 & -u & 0 \end{bmatrix}$$

$$\mathbf{b}_v = \begin{bmatrix} I_y - \frac{\rho}{2} l^5 M_{\dot{q}} & 0 & 0 \\ 0 & 1 & 0 \\ 0 & 0 & 1 \end{bmatrix}^{-1} \begin{bmatrix} \frac{\rho}{2} l^3 U^2 N_{\delta_S} \\ 0 \\ 0 \end{bmatrix}$$

$$\mathbf{x}_v = \begin{bmatrix} q & \theta & z \end{bmatrix}^{\mathbf{T}}$$

Placing the sliding poles of the system at [0 - 2.5 - 2.4], we got the diving control law as:

$$\delta_S = 0.4414q + 0.5309\theta + 4\eta \tanh\left(q + 4\theta - 4\left(z - z_{com}\right)/0.65\right) \tag{9}$$

The line of sight (LOS) is the horizontal plane angle for the guidance function of ISiMI. It was derived from:

$$\psi_{com} = \tan^{-1}\left[\frac{\left(Y_k - Y(t)\right)}{\left(X_k - X(t)\right)}\right] \tag{10}$$

in which $\begin{bmatrix} X_k & Y_k \end{bmatrix}$ are the waypoints preprogrammed in the vehicle, and $\begin{bmatrix} X(\mathrm{t}) & Y(\mathrm{t}) \end{bmatrix}$ is the current location of the vehicle. The decision as to whether or not the waypoint has been reached is made from:

$$\rho^2(t) = \left[Y_k - Y(t)\right]^2 + \left[X_k - X(t)\right]^2 < \rho_0^2 \quad 0 < \lambda < 1 \tag{11}$$

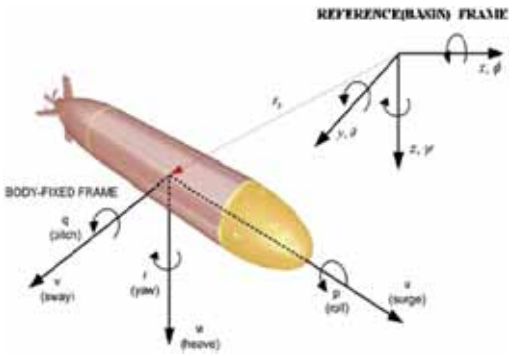

Fig. 9. Coordinate frame

5. Free running tests in the OEB

A series of free running tests of ISiMI was carried out in the OEB. The test was intended to determine ISiMI's maneuvering characteristics and to validate its basic functions as a test-bed AUV. The results might be used as references for the design of high-level control algorithms such as path planning or of the guidance system of ISiMI. ISiMI was easily launched without any special device, as shown in Fig. 10. The image tracking system of CPMC gathered the velocity and position of ISiMI during the free running test.

5.1 Advanced speed test

An advanced speed test was carried out, and the fulfillment of the design speed was verified. The advanced speed of ISiMI with respect to the propeller's rpm was determined, as shown in Fig. 11. The design speed (1 m/s) was reached at a propeller speed of about 1,000 rpm. By extrapolating the results shown in Fig. 11, it is estimated that the maximum speed (2 m/sec) was reached at 1,650 rpm.

Fig. 10. Launching and recovery of ISiMI in the OEB.

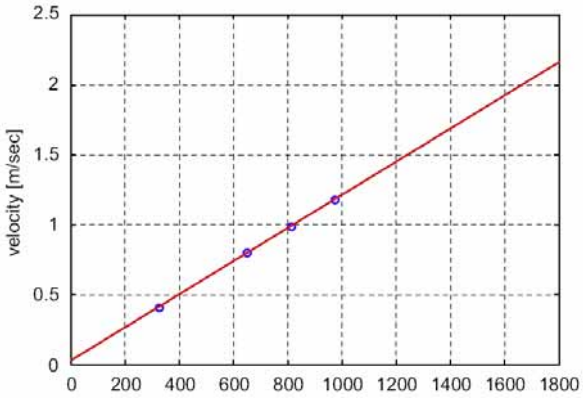

Fig. 11. Advanced speed test of ISiMI.

5.2 Open-loop zigzag test

The zigzag test was conducted to check the horizontal maneuvering property of ISiMI. The results of the test in the horizontal plane were plotted with the simulation results conducted

with the 6-DOF non-linear model in Fig. 12. The velocity of ISiMI was 0.8 m/sec and its rudder angle was toggled between -12.6 degrees and +12.6 degrees. The experimental results showed that the overshoot angle was in the range of 5~7.6 degrees. The hydrodynamic coefficients used in the simulation are listed in (Jun et al., 2008). The discrepancy between the simulation and experiment results shows that the numerical model has more yaw damping or less fin force than ISiMI. The experimental results will be used in system identification for the correction of the numerical model in future works.

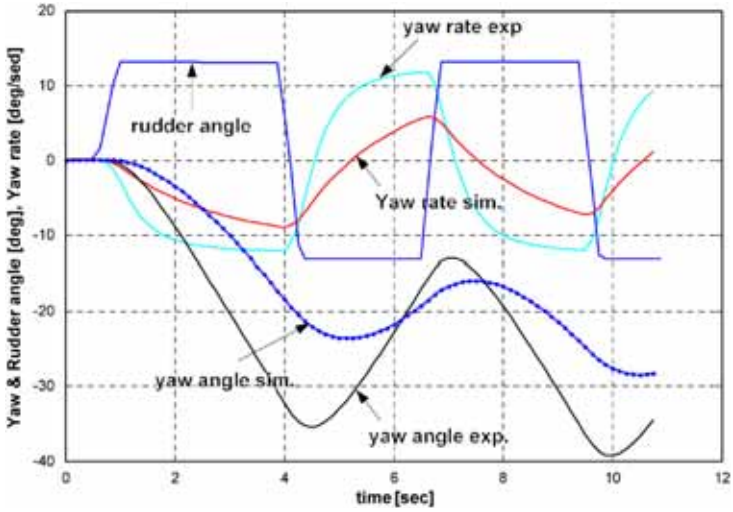

Fig. 12. Experimental results of open-loop zigzag test.

5.3 Open-loop turning test

To calculate ISiMI's turning radius, a turning test was carried out. The test results are plotted in Fig. 13, from which the turning characteristics of ISiMI were analyzed. The steady turning radius was about 6 m, and the steady turning speed and rate were about 0.6 m/sec and -6 degrees/sec when the rudder angle was 15 degrees at the advanced speed of 0.7 m/sec.

5.4 Closed-loop depth control

As the basic functions of an AUV test-bed, the depth control and waypoint tracking control functions were tested. A sliding mode controller was designed and tested for ISiMI's depth control. The experimental results are plotted with the simulation results of the linear and non-linear models in Fig. 14. The initial depth was 0.4 m, and the reference depth was 1 m. Both the experimental and simulated results showed good convergence with the reference depth. The settling time of the experiment results was longer, however, than that of the simulation results, and the amplitude of the pitch rate response in the simulation was larger than that in the experiment results. It is supposed that the discrepancies in the responses are due to the errors of the numerical and real model in pitch motion. A more exact numerical model will be estimated based on the experimental data using the system identification method in future works.

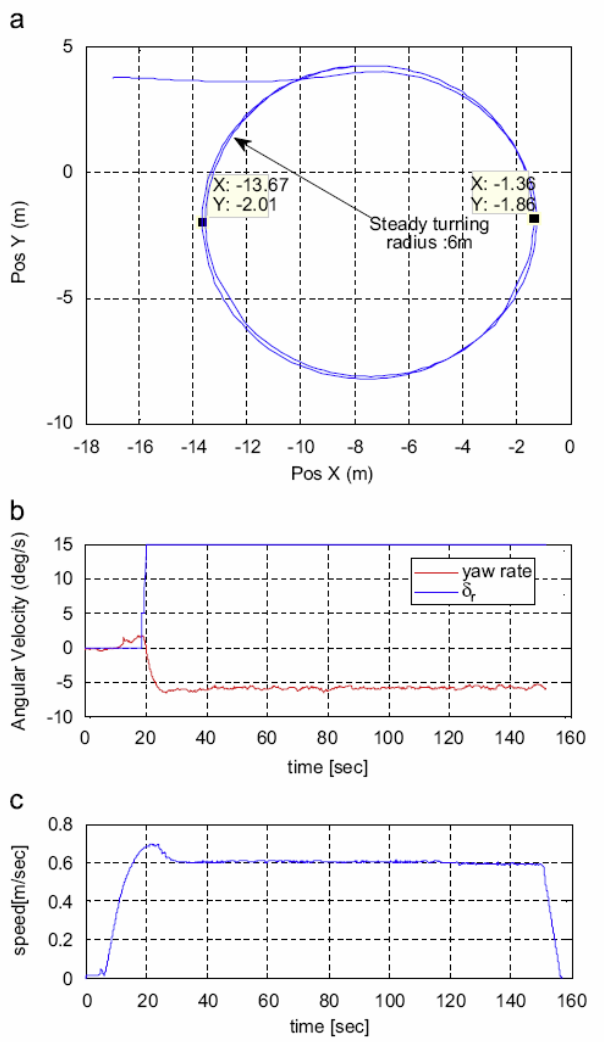

Fig. 13. Experimental results of open-loop turning test: (a) turning radius; (b) steady state turning rate and (c) steady state turning speed.

5.5 Waypoint tracking

ISiMI was guided to track a figure-eight trajectory to test the LOS algorithm described in Section 4.2. The position of ISiMI was measured using the image tracking system in CPMC, and transmitted to ISiMI via the R/F link. The position of the waypoints was pre-recorded in ISiMI's memory. The threshold level ρ_o in (11) was 1 meter. The results are plotted in Fig. 15. The yaw angle in Fig. 15 was controlled by the PD controller to follow the yaw reference generated by the LOS. It was verified that waypoint tracking, the basic function of the test-bed, was successfully achieved.

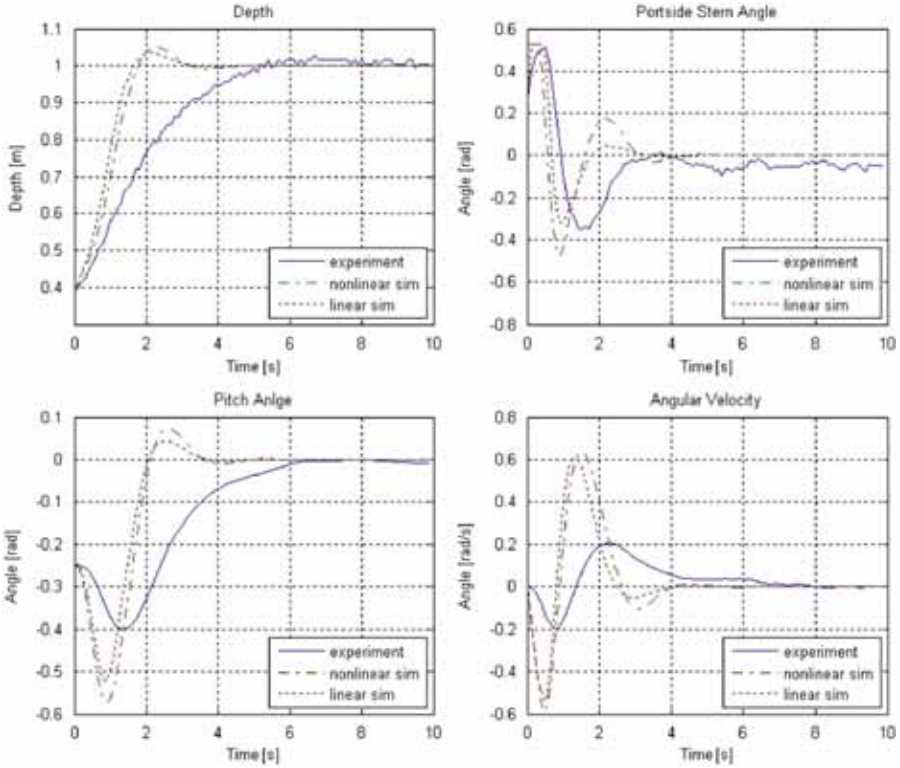

Fig. 14. Experimental results of close-loop depth control with sliding mode control.

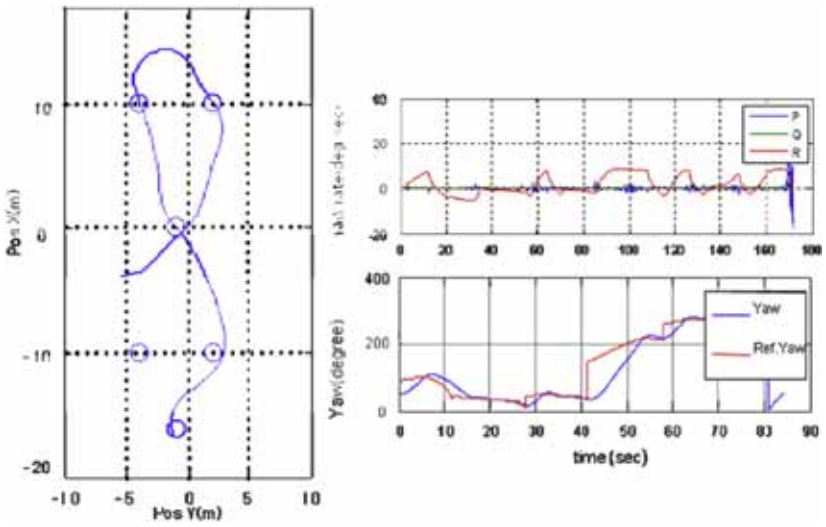

Fig. 15. Experimental results of waypoint tracking.

6. Image processing

In this chpater, image processing means detecting and discriminating the location of the lights on the dock and estimating relative position and distance between the AUV and the dock.

Figure. 16 shows a developed dock and the arrangement of the lights in the entrance of the dock. The diameter of the rim was 1m. Five lights were installed in the circular rim. The locations and brightness of the lights were adjustable. Before the image processing, it was necessary to adjust the intensity of the lights. If the lights is too strong, two or more lights may be misidentified as one light because of scattering. Proper intensity was determined through trial-and-error.

Figure 17 shows the coordinates of the vision system. The origin of the camera coordinate is at the center of the nose. The image coordinate is coincident with the camera coordinate except for the x-directional shift f (focus length).

The processing consists of 4 stages. (1) Image grabbing, (2) Binarization of the grabbed images, (3) Elimination of noisy luminaries and discrimination of the dock lights and (4) Estimation of the position and a distance of the dock center.

Stage (1) Raw images were grabbed. Lights were scattered, and this scattering made finding the exact positions of the light sources difficult.

Stage (2) To discriminate the lights installed around the dock entrance, the image processing unit classified each pixel of the raw images into two groups (a bright group and a dark group) using a pre-specified threshold value. Namely, the grabbed image was converted into a binary image. The lights of the dock were classified as the bright group, and the background became the dark group. In this process, salt-and-pepper noise was produced. Salt-and-pepper noise is the presence of single dark pixels in bright regions, or single bright pixels in dark regions. This is the natural result of creating a binary image via thresholding (Shapiro, 2001). This noise was removed using 3pixel by 3pixel masks. Appropriate size for the mask was determined by trial-and-error. After a pixel was classified in the bright group, the distance between that pixel and the nearest white pixel was investigated to identify each of the lights. If the distance was shorter than a pre-specified range, it was supposed that those two pixels belonged to one light region. If not, it was supposed that those two pixels belonged to two separate lights

Stage (3) Underwater, there were noisy luminaries that had to be eliminated. The luminaries are shown in Fig. 18. Some of the luminaries emitted light with an intensity similar to that of the dock lights. In such cases, ISiMI could be confused. Two particular problems were the presence of several lamps outside of the basin, and the fact that the dock lights were reflected back down from the surface of the water. Because these luminaries were interfered with the upper portion of the dock, they could be eliminated by processing the image frame from the lower-right pixel to the upper-left pixel. The processing was ended after five bright regions were acquired. All of the five lights had to be detected, i.e. the image processing required detection of all five lights. If one or more lights could not be detected, the image processing would fail. This was a defect of the developed processing. Stage (2) and Stage (3) were executed simultaneously. Due to Stage (2) and Stage (3), the dock lights were identified. Once the five dock lights were detected, a local searching area was generated and the image processor considered only this area in the next step.

Stage (4) From positions of the lights identified in the image coordinates, ISiMI estimated the position and the distance to the dock center. The center of the dock was calculated by

averaging the coordinates of the five lights. To estimate the distance, the number of white pixels in Light #5 was counted (Fig. 16). Because Light #5 was located relatively far from others, interference from scattering was relatively small. The distance information was used as one threshold to decide whether vision-guidance was valid or not.
If the coordinate of the n-th light is P_n then the center of the dock is given by

$$P_C(z) = \frac{\sum_{n=1}^{5} P_n(z)}{5}$$
$$P_C(y) = \frac{\sum_{n=1}^{5} P_n(y)}{5} \tag{12}$$

Fig. 19 shows the sequence of the introduced image processing. From the left, the raw image (left) and the binary image (center) are shown. There are some noisy luminaries that must be eliminated in the upper portion. The five white points in the lower portion are the dock lights. The last photograph (right) is a processed image. It shows elimination of the noisy luminaries and discrimination of the dock lights. The detected lights of the dock are marked by squares. The estimated center of the dock is also marked.

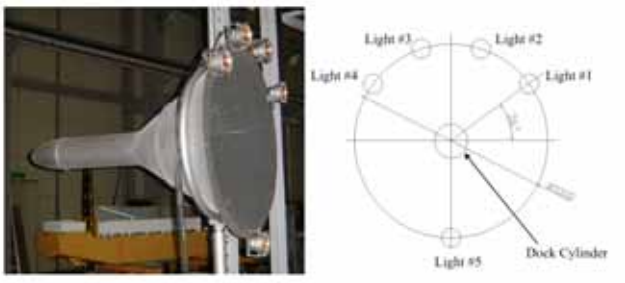

Fig. 16. The docking device with five lights around the rim of the entrance: The location and intensity of the lights is adjustable. (Left) Photo of the dock configuration and (Right) arrangement of the lights.

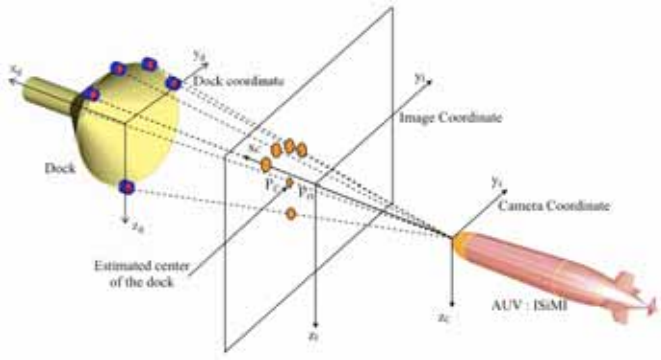

Fig. 17. Coordinates of the vision system.

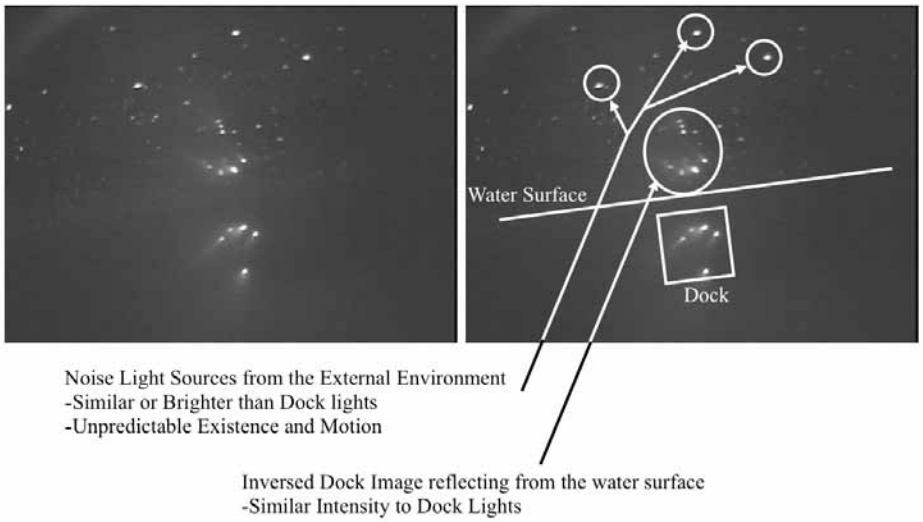

Fig. 18. Raw Image (left) and Noisy Luminaries (right): Several lamps were outside of the basin, and the dock lights are reflected down from the water surface.

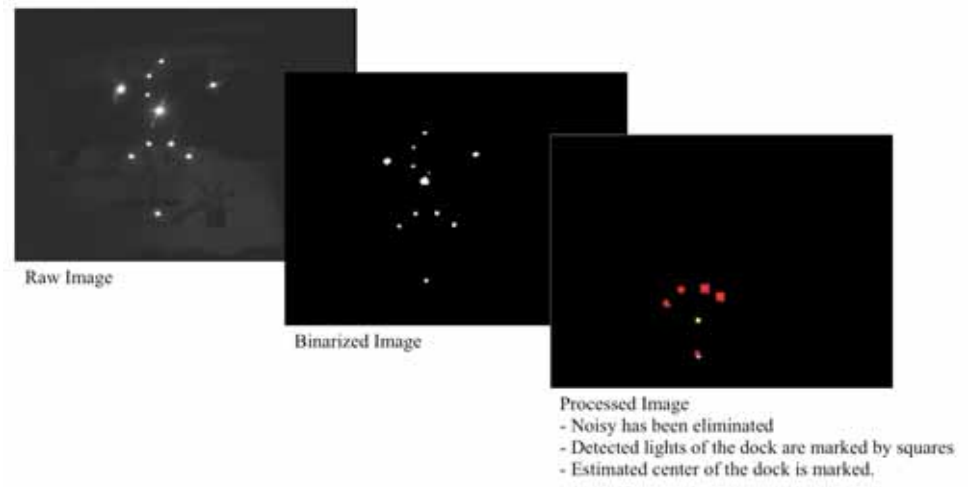

Fig. 19. Image process sequence (test screenshots was used): Raw image (left), binary image- some noisy luminaries remain. (center), and processed image - elimination of noisy luminaries and discrimination of the dock lights.

7. Final approach algorithm

It was first suggested by Deltheil et al (2000) that a vision system is suitable for docking because it offers simplicity, stealthiness and robustness. In this chapter, a final approach algorithm based on vision-guidance is suggested. It was supposed that the AUV could be

guided to the dock by controlling only yaw and pitch. This final approach algorithm generates reference yaw and reference pitch and makes the AUV track them.
The docking stage begins when the AUV arrives within 10-15 m in front of the dock. The docking stage of the return process is subdivided here into two stages because there exists an area where the dock lights are out of the camera viewing range when the AUV is close to the dock. Figure 20 shows the first and second stages. During the second stage the AUV is about 1.4m from the dock, and the lights of the dock are out of the range of the camera. The essential difference of the second stage is the manner of generating reference yaw for steering motion and reference pitch for diving motion. During both parts of the docking stage, a conventional Proportional-Derivative (PD) control is applied to track the references. Values of these gains were tuned by trial-and-error using the results of the simulations and underwater experiments.
A. The first stage
In this stage, reference yaw and pitch were generated based on vision-guidance. All dock lights were located in the viewing range of the CCD camera. This vision-guidance controller generated reference yaw and reference pitch using the estimated center of the dock. A discrepancy between the estimated dock center and the origin of the image coordinates became an error input of the vision-guidance controller. Fig. 21 is a block diagram of the vision-guidance control. A Proportional-Integral (PI) controller was used to generate reference yaw and pitch from the position error. To eliminate steady-state error, I-control was used. By conducting repeated underwater experiments, values of the PI gains were tuned.

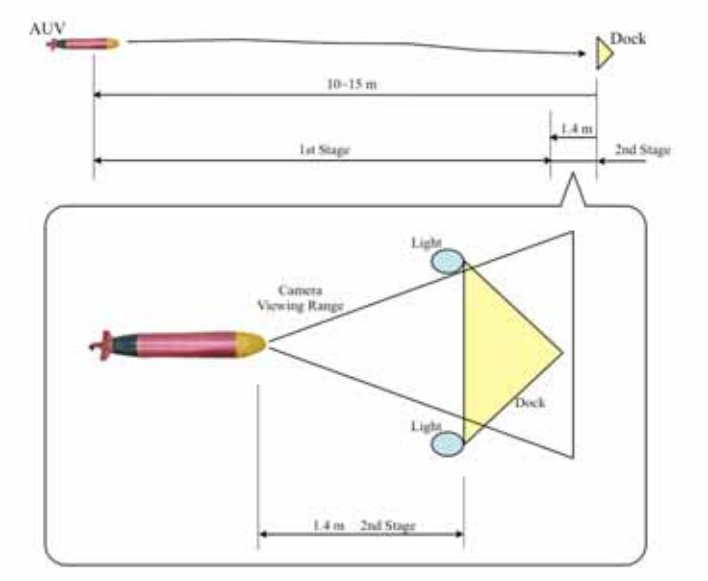

Fig. 20. The 1st stage and the 2nd stage of docking approach

B. The second stage
When the distance estimated by the image processing became smaller than a pre-specified threshold value, the second stage began. In this area, the last reference yaw and pitch

become fixed. Because the AUV is very close to the dock, it was supposed that changing yaw or pitch could be dangerous and keeping the final references would be plausible. This method is referred to as 'attitude keeping control.' (Park et al., 2007) During this phase, ISiMI becomes blind and simply tracks these final fixed references until contacting the dock. Fig. 22 shows a flow chart of the final approach algorithm.

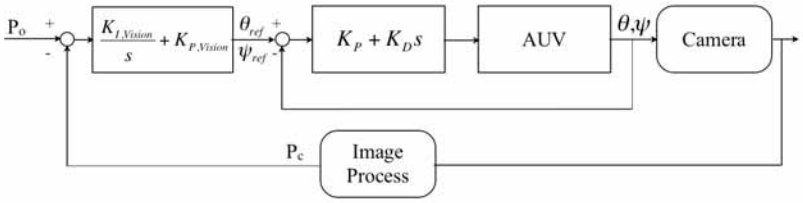

Fig. 21. The vision-guidance control algorithm. P_o is the origin of the image coordinate frame. P_c is the estimated center of the dock. θ is pitch, ψ is yaw. θ_{ref} and ψ_{ref} are generated reference pitch and yaw, respectively.

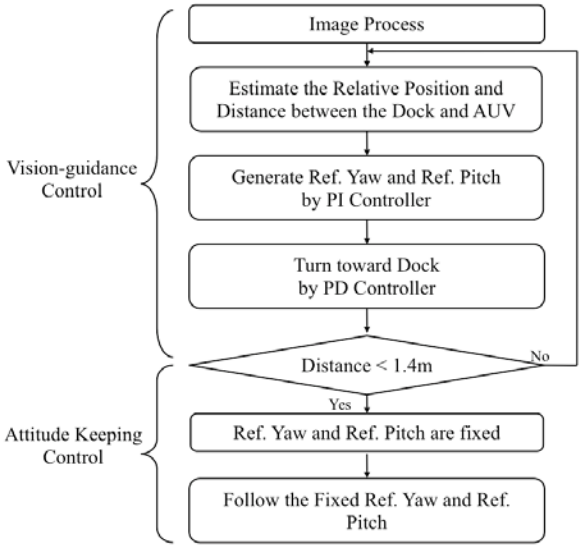

Fig. 22. Flow chart of the final approach algorithm.

8. Underwater docking experiments

The goal of the experiments was to verify the final approach algorithm and system validity. Figure 23 describes the initial start point for the final docking approach. It shows a top view (left) and a side view (right) of the initial start conditions. The dock was placed within viewing range of the camera. The center of the dock was placed at a depth of 1.5m. The dock was introduced by (Lee et al, 2003), (Park et al, 2007). The dock was funnel-shaped. This shape makes it possible for the AUV to dock successfully through sliding even if she approaches obliquely. The dock used an external power source.

Because robustness against disturbance has not yet been developed and this attempt was during the early stages of development, some restrictions were applied. There was no current and there were no waves. The dock was fixed on the basin floor. The water was clean. ISiMI was operated using a wired LAN communication. RF wireless communication was not suitable to receive the large amount of image data necessary. The wireless LAN was disconnected when the AUV submerged. The R.P.M. of the thrust propeller was invariant and the forward speed was about 1.0m/s. The relation between R.P.M and speed was determined by (Jun et al. 2008). There was no speed control. Experiments without the attitude keeping control and experiments with the attitude keeping control were conducted separately.

A. Underwater docking experiment without the attitude keeping control

Only the vision-guidance control was applied. No distance estimation was applied. ISiMI depended on the camera until contact with the dock. In Fig. 24, pixel errors are plotted against time. A pixel error is defined as deviation between the origin and the estimated center of the dock center in the image coordinate. The pixel errors decreased and were regulated during the first 9 seconds of the test. However, between seconds 9-15, there were discontinuous oscillations. These oscillations were caused by the defect of the image processing system to process, not by actual motions of the AUV, i.e. one more light moved out of the camera viewing range. The AUV became confused and it could not find the center of the dock. This occurred when the AUV was in the second stage area. To estimate the center precisely, all five lights were required, but in this area, the AUV could not see all of them. It was found that the AUV had some head-on collisions with Light #5 or the inner plane of the dock. She performed imprecise final approaches and suffered collisions with the dock. Fig. 25 is a sequence of continuously grabbed images taken by an underwater camera. (a) ISiMI starts, (b) she cruises to (c) the dock, (d) an imprecise approach near the dock, (e) after a collision, she rebounded and (f) she could not enter the dock. Thus, it was proven that the vision-guidance control was not unnecessary during this part of the docking procedure.

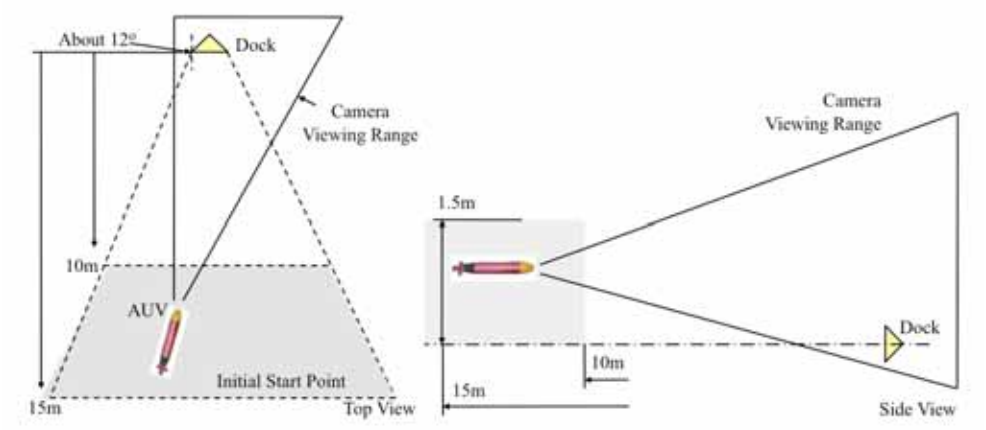

Fig. 23. Initial start point: (left) top view and (right) side view

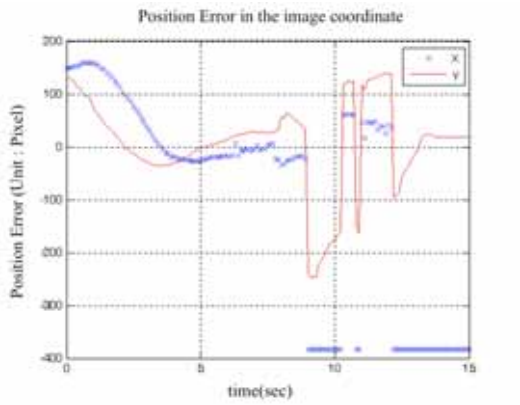

Fig. 24. Position error (unit: pixel) in the image coordinate. The vision-guidance control was applied through all intervals. (1) t = 0-9seconds : Errors are decreasing. In this interval, all 5 lights were in the viewing range of the camera. The AUV was able to estimate the center precisely. (2)t = 9-15seconds : one or more lights were out of the viewing range of the camera. Precise estimation of the center became impossible. The oscillation was caused by the defect of information from image processing rather than actual motion of the AUV.

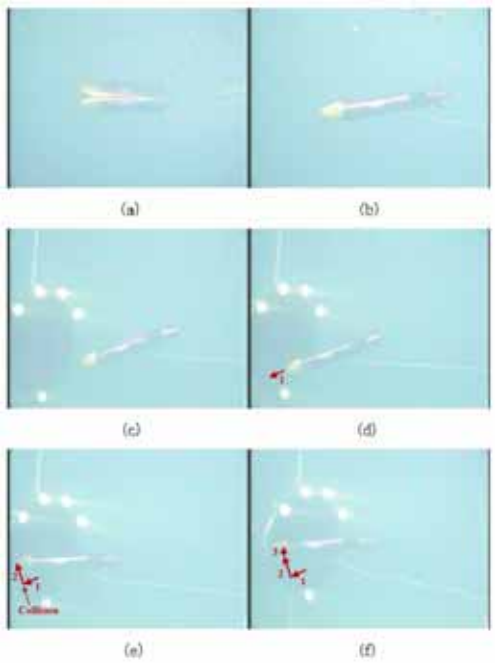

Fig. 25. Docking : Grabbed images by an underwater camera (Arrows indicate moving directions of the AUV): (a): ISiMI starts, (b): She cruises to (c) the dock, (d): An imprecise approach near the dock, (e): After a collision, she rebounded, and (f): She could not enter the dock.

B. Underwater docking experiment with the attitude keeping control
The attitude keeping controller was applied when ISiMI was near the dock. Image processing was used to estimate both the location of the center and the distance to the dock. The patterns were similar to that of Fig. 24 during the first 9 seconds of the test. Oscillations of the sort encountered during the first test were anticipated after 9 seconds. However, after the vision-guidance control was stopped, the reference yaw and pitch were fixed by the attitude keeping controller. In Fig. 26, the solid lines are the yaw(the upper graph) and pitch(the lower graph) measured by AHRS. The short-dash lines are the generated reference yaw and pitch. After 9 seconds, the references were fixed. The long-dash lines show the fixed references and the AUV tracked them. Fig. 27 shows the moment of docking. The

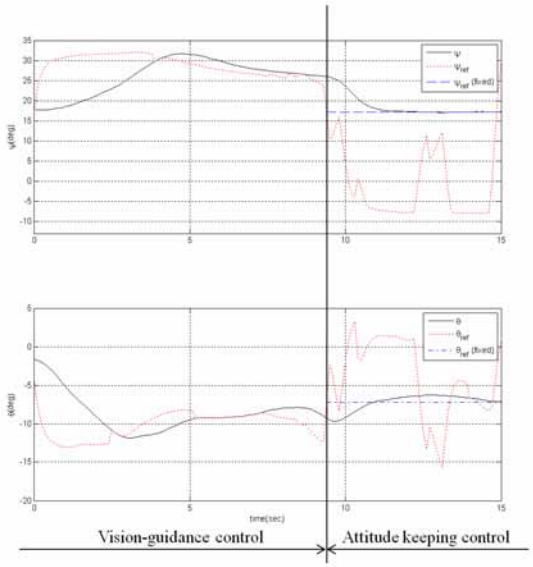

Fig. 26. Final approach: (upper) Yaw, Ref. yaw and fixed ref. yaw (lower) Pitch, Ref. pitch and fixed ref. pitch are shown respectively. After 9 seconds, ref. yaw and ref. pitch were fixed. (1)t = 0-9seconds : The vision-guidance control was applied. In this interval, all 5 lights were in the viewing range of the camera. (2)t = 9-15seconds : At t = 9.4seconds, the attitude keeping control began and the references were fixed.

Fig. 27. Docking: (left) The original photograph. The original photograph was sharpened anad the edge of ISiMI was emphasized to make her more easy to recognize. The white arrow indicates ISiMI (right).

original photo was sharpened and the edge of IsiMI was emphasized in order to make her more easy to recognize. The photo shows that ISiMI was going into the dock with a more precise approach.

9. Conclusion

In this chpater, the design, implementation and test results of a small AUV named ISiMI are presented. The AUV, ISiMI, developed in KORDI is a test-bed for the validation of the algorithms and instruments of the AUV. For fast experimental feedback on new algorithms, ISiMI was designed to be able to cruise in the Ocean Engineering Basin environment at KORDI. The zigzag test and the turning test were carried out to check ISiMI's maneuvering properties. The depth control and waypoint tracking tests were carried out to validate the feedback controller of ISiMI. The experiment results were compared with those of the simulation. The research works were fed back to the design and implementation of a 100m-class AUV named ISiMI100. ISiMI100 is equipped with additional sensors such as a doppler velocity log, an acoustic telemetry modem, an obstacle avoidance sonar, a range sonar, and a GPS module. A photo of ISiMI100 is shown in Fig. 28. The mission test of ISiMI and the sea trial of ISiMI100 remain to be performed in future works.

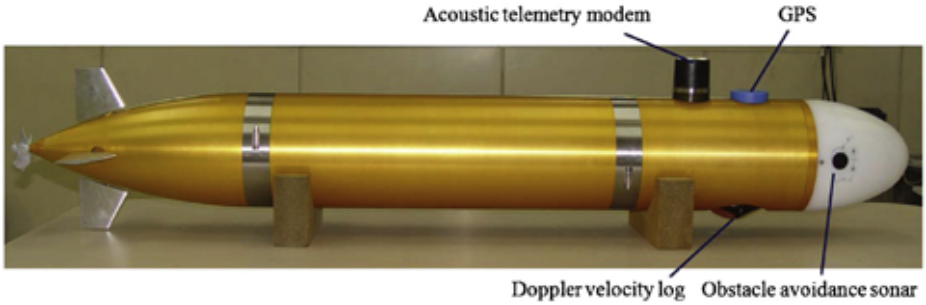

Figure 28. Sea-trial version of ISiMI AUV named ISiMI100

A final approach algorithm based on vision guidance for the underwater docking of an AUV was developed and introduced. The algorithm allowed the tested AUV to identify dock lights, eliminate interfering luminary noises and successfully estimate both the center of the dock and the distance to it during the first stage of the docking sequence despite the fact that the AUV was unable to detect the dock lights when close to the dock. The final approach algorithm based on vision guidance did guide the AUV to the dock successfully. The area where the lights were out of the camera viewing range occasioned confusion, as expected, but the attitude keeping control was able to keep the AUV on the way to the dock. Underwater docking experiments showed the necessity of the attitude keeping control. The use of the attitude keeping control as well as the vision-guidance control improved the precision of docking performance. The fixed references guided the AUV more precisely and safely. Although the docking experiments were conducted under controlled conditions, the results of the experiments showed the utility and potential of the vision-based guidance algorithm for docking.

Future problems include successfully docking when (1) the dock is moving, (2) the dock is placed out of the camera viewing range at the beginning of a return process, and (3) currents

and waves are present. Generation of the optimized path from any initial start point to the dock is also a subject for future study.

10. Acknowledgments

This work was supported in part by MLTMA of Korea for the "development of a deep-sea unmanned underwater vehicle," and KORDI, for the "development of ubiquitous-based key technologies for the smart operation of maritime exploration fleets."

11. References

Allen, B., Stokey, R., Austin, T., Forrester, N., Goldsborough, R., Purcell, M., von Alt, C., 1997. REMUS: A small, low cost AUV; system description, field trials and performance results. Proceedings of the Oceans Conference pp 994-1000.

Allen, B., Austin, T., Forrester, N. Goldsborough, R. Kukulya, A., Packard, G., Purcell. M., Stokey, R., 2006. Autonomous docking demonstrations with enhanced REMUS technology, Proceedings of OCEANS 2006. MTS/IEEE, pp. 1-6.

Bellingham, J.G., Bales, J.W., Goudey, C.A., Consi, T.R., 1993. Performance characteristics of the Odyssey AUV. Proceedings of the Eighth International Symposium on Unmanned Untethered Submersible Technology (AUV '93), pp. 37-59.

Cowen, S., Briest, S., Dombrowski, J., 1997. Underwater docking of autonomous undersea vehicles using optical terminal guidance, Proceedings of OCEANS '97. MTS/IEEE, Vol. 2, pp. 1143-1147.

Deltheil, C., Didier, L., Hospital, E., Brutzman, D. P., 2000. Simulating an optical guidance system for the recovery of an unmanned underwater vehicle, IEEE Journal of Oceanic Engineering, Vol. 25, No. 4, pp. 568-574.

Edwards, D.B., Bean, T.A., Odell, D.L., Anderson, M.J., 2004. A leader-follower algorithm for multiple AUV formations. Proceedings of IEEE/OES. pp 40-46.

Feezor, M. D., Blankinship, P. R., Bellingham, J. G., Sorrell, F. Y., 1997. Autonomous underwater vehicle homing/docking via electromagnetic guidance, Proceedings of OCEANS '97. MTS/IEEE, Vol. 2, pp. 1137-1142.

Feldman, J., 1979. DTNSRDC Revised Standard Submarine Equations of Motion. DTNSRDC/SPD-0393-09.

Fiorelli, E., Leonard, N.E., Bhatta, P., Paley, D., Bachmayer, R., Fratantoni, D.M., 2004. Multi-AUV control and adaptive sampling in Moterey Bay. Workshop on Multiple AUV Operations (AUV04). pp 134-147

Fossen, T.I., 1994. Guidance and Control of Ocean Vehicles. John Wiley & Sons Ltd.

Gertler, M., Hagen, G. R., 1967. Standard equations of motion for submarine simulations, NSRDC Report No. 2510.

Healey, A.J., Lienard, D., 1993. Multivariable sliding-mode control for autonomous diving and steering of unmanned underwater vehicles. IEEE Journal of Oceanic Engineering, 18 (3), 327-339.

Hobson, B. W., McEwen, R. S., Erickson, J., Hoover. T., McBride, L., Shane, F., Bellingham, J. G., 2007. The development and ocean testing of an AUV docking station for a 21" AUV, Proceedings of OCEANS 2007.

Hong, Y. H., Kim, J. Y., Lee, P. M., Jeon, B. H., Oh, K. H., Oh, J. H., 2003. Development of the homing and docking algorithm for AUV, Proceedings of the Thirteenth International Offshore and Polar Engineering Conference, pp. 205-212.

Jeon, B.H., Lee, P.M., Li, J.H., Hong, S.W., Kim, Y.G., Lee, J., 2003. Multivariable optimal control of an autonomous underwater vehicle for steering and diving control in variable speed, Proceedings of Oceans Conference, San Diego, pp 2659-2664.

Jun, B. H., Park, J. Y., Lee, P. M., Ma, S. J., Kim, Y. S., Oh, J. H., Lim, Y. K., 2007. Design, implementation and free running test of ISiMI; an AUV for cruising in ocean engineering basin environment, Proceedings of OCEANS 2007 IEEE Aberdeen.

Jun, B. H., Park, J. Y., Lee, F. Y., Lee, P. M., Lee, C. M., Kim, K. H., Lim, Y. K., Oh, J. H., 2008. Development of the AUV 'ISiMI' and a free running test in an Ocean Engineering Basin, Ocean Engineering, http://dx.doi.org/10.1016/j.oceaneng.2008.07.009

Kim, J. Y., Park, I. W., Oh. J. H., 2006. Experimental realization of dynamic walking of the biped humanoid robot KHR-2 using zero moment point feedback and inertial measurement, Advanced Robotics, Vol. 20, No. 6, pp. 707-736.

Lee, P. M., Hong, S.W., Lim, Y.K., Lee, C.M., Jeon, B.H., Park, J.W, 1999. Discrete-time quasi-sliding mode control of an autonomous underwater vehicle. IEEE Journal of Oceanic Engineering, 24 (3), 388-395.

Lee, P. M., Jeon, B. H., Lee, C. M., 2002. A docking and control system for an autonomous underwater vehicle, Proceedings of OCEANS 2002. MTS/IEEE, pp. 1609-1614.

Lee, P. M., Jeon, B. H., Kim, S. M., 2003. Visual servoing for underwater docking of an autonomous underwater vehicle with one camera, Proceedings of OCEANS 2003, Vol. 2, pp. 677-682.

Lee, P. M., Jun, B. H., Kim, K. H., Lee, J. H., Aoki, T., Hyakudome, T., 2007. Simulation of an inertial acoustic navigation system with range aiding for an autonomous underwater vehicle. IEEE Journal of Oceanic Engineering, 32 (2), 329-345.

Lee, P. M., Jun, B. H., 2007. Pseudo long base line navigation algorithm for underwater vehicles with inertial sensors and two acoustic range measurements, Ocean Engineering, Vol. 34, Issues 3-4, pp. 416-425.

Myring, D. F., 1976. A theoretical study of body drag in subcritical axisymmetric flow, Aeronautical Quarterly, vol. 27, pp 186-194.

Nerstein W., Smith, K.C., 1968. Hydrodynamic coefficient equations and computer programs. The bendix Corporation report.

Park, J. Y., Jun, B. H., Lee, P. M., Lee, F. Y., Oh, J. H., 2007. Experiment on underwater docking of an autonomous underwater vehicle 'ISiMI' using optical terminal guidance, Proceedings of OCEANS 2007 IEEE Aberdeen.

Prestero, T., 2001. Verification of a Six-Degree of Freedom Simulation Model for the REMUS Autonomous Underwater Vehicle. M.S. Dissertation, MIT and WHOI.

Shapiro, L. G., Stockman, G. C, 2001. Computer Vision, Prentice Hall, NJ.

Singh, H., Bellingham, J.G., Hover, F., Lerner, S., Moran, B.A., Heydt, K., Yoerger, D., 2001. Docking for an autonomous ocean sampling network. IEEE Journal of Oceanic Engineering, 26 (4), 498-514.

Stokey, R., Allen, B., Austin, T., Goldsborough, R., Forrester, N., Purcell, M., Alt, C.V., 2001. Enabling technologies for REMUS docking : an integral component of an autonomous ocean-sampling network. IEEE Journal of Oceanic Engineering, 26 (4), 487-497.

Utkin, V.I., 1977. Variable structure system with sliding modes. IEEE Transactions on Automatic Control, 22 (2), 212-222.
http://auvlab.mit.edu/vehicles/vehiclespecEARLY.html#OD1
http://www.gavia.is/downloads/brochures/GaviaBrochure0402.pdf